DOI 10.4430/bgo00346

Modified Particle Swarm Optimisation (MPSO) for inversion of gravity field due to simple causative mass

A. Eshaghzadeh[1] and S. Seyedi Sahebari[2]

[1] *Department of Geology, Faculty of Sciences, University of Isfahan, Isfahan, Iran*
[2] *Department of Engineering, University College of Nabi Akram, Tabriz, Iran*

(Received: 1 July 2020; accepted: 11 November 2020; published online: 20 September 2021)

ABSTRACT Modified Particle Swarm Optimisation (MPSO) is an improved algorithm of Particle Swarm Optimisation (PSO), where the learning factors or acceleration coefficients *(c_1* and *c_2)* and inertia weight (*w*) change during iteration as ability of finding the optimal solution can be enhanced. In the MPSO algorithm, a new concept of the velocity of the individual (particle) modification, the evolution of the particle best value (*Pbest*) and global best value or best value in the group (*Gbest*), is presented as an acceptable convergence in the MPSO algorithm solutions is found. An advantage of the MPSO over the PSO is that it does not stick: it does not stick to a local minimum giving, then, a premature convergence. We have tested the proficiency of the MPSO and PSO using the theoretical gravity caused by buried sources with simple geometry, such as spheres, horizontal cylinders, and vertical cylinders, with and without added random noise. In comparison with the PSO algorithm, the MPSO inversion gives the most satisfactory results for the noise-free and noise-corrupted theoretical gravity data. We have also applied the MPSO approach for inverse modelling of the five residual gravity anomalies due to various causative mass from the different parts of the world, as the estimated results are compared with other previous researches.

Key words: residual gravity, Modified Particle Swarm Optimisation (MPSO).

1. Introduction

Non-uniqueness is a feature in the linear inverse modelling of residual gravity anomalies. This feature could assign a set of the measured gravity field data on the ground surface to the several geometrical distributions of the subsurface mass with various shapes and physical parameters such as density and depth. One way to eliminate this ambiguity is to set a suitable geometry on the anomalous body with a known density followed by inversion of gravity anomalies (Chakravarthi and Sundararajan, 2004). Although considering models with simple geometric shapes may not be geologically realistic, they are usually sufficient to analyse sources of many isolated anomalies (Abdelrahman and El-Araby, 1993a, 1993b). The interpretation of such an anomaly aims essentially at estimating the parameters such as shape, depth, and radius of the gravity anomaly causative body such as geological structures, mineral mass and artificial underground structures.

Several graphical and numerical methods have been developed to analyse residual gravity anomalies caused by simple bodies, such as Saxov and Nygaard (1953) and Bowin *et al.* (1986). The methods include, for example, Fourier transform (Odegard and Berg, 1965; Sharma and Geldart,

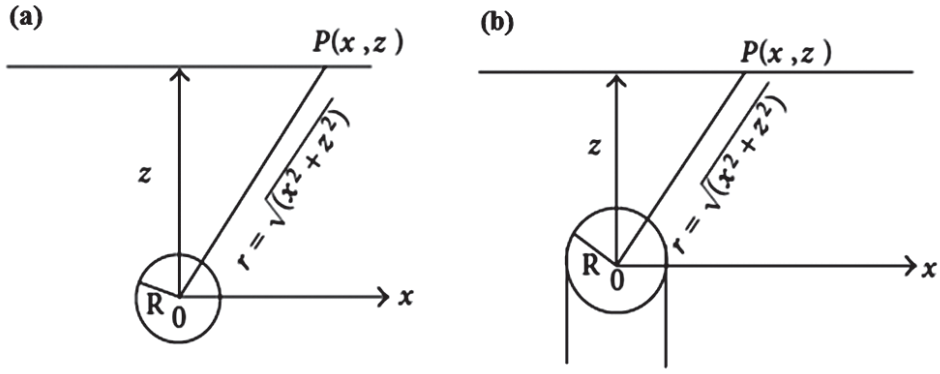

Fig. 1 - a) Sphere and infinite horizontal cylinder models, b) semi-infinite vertical cylinder model.

1968), Mellin transform (Mohan *et al.*, 1986), Walsh transforms techniques (Shaw and Agarwal, 1990), ratio techniques (Hammer, 1977; Abdelrahman *et al.*, 1989), least-squares minimisation approaches (Gupta, 1983; Lines and Treitel, 1984; Abdelrahman, 1990; Abdelrahman *et al.*, 1991), different neural networks (Eslam *et al.*, 2001; Osman *et al.*, 2006, 2007; Al-Garni, 2013; Eshaghzadeh and Kalantari, 2015; Eshaghzadeh and Hajian, 2018), and effective quantitative interpretations using the least squares method based on the analytical expression of simple moving average residual gravity anomalies (Gupta, 1983). Abdelrahman and El-Araby (1993a, 1993b) introduced an interpretive technique based on fitting simple models convolved with the same moving average filter as applied to the measured gravity. A simple method proposed by Essa (2007) is used to determine the depth and shape factor of simple shapes from residual gravity anomalies along the profile. Another automatic method, the least squares method, was proposed by Asfahani and Tlas (2008), by which the depth and amplitude coefficient can be determined. Eshaghzadeh *et al.* (2020) developed a simultaneous nonlinear inversion based on the Marquardt optimisation to estimate the radius and depth parameters of the buried structures with simple geometry from gravity data.

Particle Swarm Optimisation (PSO) is a relatively recent method and one of the most popular nature-inspired heuristic optimisation algorithms developed by Kennedy and Eberhart (1995). PSO has few applications for geophysical problems (Alvarez *et al.*, 2006; Shaw and Srivastava, 2007). However, PSO has been successfully employed in some fields of geophysics, such as inversion of self-potential of idealised bodies' anomalies (Monteiro Santos, 2010), gravity inversion of a fault by PSO (Toushmalani, 2013a, 2013b), gravity inversion and uncertainty assessment of basement relief via PSO (Pallero *et al.*, 2015), application of PSO for gravity inversion of 2.5D sedimentary basins (Singh and Singh, 2017), 2D dipping dike magnetic data interpretation using a robust PSO (Essa and El-Hussein, 2017), inversion of residual gravity anomalies using tuned PSO (Roshan and Singh, 2017), gravity data interpretation using PSO (Essa and El-Hussein, 2018a, 2018b), and PSO to interpret magnetic anomalies caused by simple geometrical structures (Essa and El-Hussein, 2018a, 2018b).

In this paper, we have proposed the Modified Particle Swarm Optimisation (MPSO) algorithm to enhance the performance of the PSO algorithm. We have applied the MPSO algorithm to estimate the buried causative mass parameters, such as depth (z), radius (R), density contrast (ρ), shape factor (q) and axis location (x_0) from the gravity anomaly. This method is examined by several noise-free and noise-corrupted synthetic gravity data, and also five real gravity data from Iran, USA, and Senegal.

2. Gravity of simple geometry

Gravity fields of many simple bodies are symmetric around the location of the source. For example, the general gravity *g* effect caused by simple models (such as a sphere, an infinite horizontal cylinder, and a semi-infinite vertical cylinder as shown in Fig. 1) at point $p(x_i, z)$ is given as (Abdelrahman *et al.*, 1989):

$$g(x_i, z, q) = \frac{K}{\left(x_i^2 + z^2\right)^q} \tag{1}$$

where *z* is the depth, *q* is a value (shape factor) characterising the nature of the source (*q* = 0.5 for a vertical cylinder, *q* = 1.0 for a horizontal cylinder, and *q* = 1.5 for a sphere) and *K* is an amplitude factor related to the radius, depth, and density contrast between the target and the surroundings ρ of the source, as:

$$K = \begin{cases} \frac{4}{3}\pi G \rho z R^3 & for\ a\ sphere \\ 2\pi G \rho z R^2 & for\ a\ horizontal\ cylinder \\ \pi G \rho R^2 & for\ a\ vertical\ cylinder \end{cases} \tag{2}$$

Here, *G* is the universal gravitational constant.

3. Modified Particle Swarm Optimization (MPSO)

MPSO is a global stochastic evolutionary algorithm based on population distribution, which is inspired by the reciprocal behaviour of the various species or individuals (called also particles) of a social such as a flock of birds, a swarm of bees, and a school of fish.

There are many references describing the performance of the PSO algorithm using the various explanations and different wording such as Monteiro Santos (2010) and Singh and Singh (2017). Here, we try to illustrate the PSO technique with the simple expressions. The PSO algorithm can be employed for optimising *N* individuals (multivariable) in a search space. Indeed, the individuals in this research are the *z*, *R*, ρ, *q*, and x_0 parameters.

Before entering into the optimisation process, it is necessary to define the initial values for the learning factors [also called acceleration coefficients (c_1 and c_2)], inertia weight (*w*) and velocity component (*V*). This terminology will be characterised subsequently. Moreover, the theoretical gravity anomaly (for synthetic models) or measured ones, the search range for each parameter, number of primary models, number of iterations and allowable error between the computed gravity anomalies and observed ones, should be determined.

The seek space for the *q* is constrained between 0.25 and 1.75 for all models ($0.25 < q \leq 1.75$). Considering the evaluated *q* using MPSO the buried mass shape is assigned where $0.25 \leq q < 0.75$, $0.75 \leq q < 1.25$, and $1.25 \leq q \leq 1.75$ indicate an under-surface structure with a form of vertical cylinder, horizontal cylinder, and sphere, respectively. The range of variations for the other model parameters is not constant and based on the geological information and qualification of the gravity field of the region under investigation.

The nonlinear inverse modelling by the PSO algorithm begins by specifying the initial models automatically based on a range of defined values for each parameter, as each model includes the values of the five parameters. These present models are also considered as the initial population or initial *Pbest* (particle best values or particle best model). Among the initial *Pbest*, the parameters of the best model or initial *Gbest* [best values (model) in the group or global best values (model)] are chosen.

Before starting the iteration process of the MPSO algorithm, a primary arbitrary speed is assigned to each of the particle (parameter), of the initial swarm. The value of each particle (parameter), as one of the potential computational variables in the MPSO algorithm, changes at each iteration of the evaluation process. In other words, this value is refreshed during the iteration so that the particle reaches its best value, which is known as *Pbest*. Accordingly, each particle attempts to adjust its value in the present velocity of the operation of the algorithm. At each iteration, the new *Gbest* is determined from the new *Pbest,* which has been estimated in the same iteration. To obtain a new value of the particle, the velocity of the particle is updated using the following equations, given by Sweilam *et al.* (2007):

$$V_i^{t+1} = wV_i^t + c_1 RAND()(Pbest_i - X_i^t) + c_2 RAND()(Gbest_i - X_i^t) \quad (3)$$

$$X_i^{t+1} = X_i^t + V_i^{t+1} \quad (4)$$

where, V_i^t is the present velocity of the individual (particle) *i* at the t_{th} iteration, X_i^t is the current position (value) of the i_{th} particle at the t_{th} iteration, *RAND*() is a random number between 0 and 1, c_1 and c_2 (learning factors) are positive constant numbers known as cognitive coefficient and social coefficient, respectively, which control the individual and the social behavior, and *w* is an inertial coefficient whose value is usually slightly less than 1 (Monteiro Santos, 2010). Generally, the *Pbest* and *Gbest* are accelerated by two operators c_1 and c_2, and two random numbers produced between [0, 1] whereas the current movement is multiplied by a *w*. In the PSO algorithm, for *w* the minimum (w_{min}) and maximum (w_{max}) limits are defined until its amount is bounded in the range [w_{min}, w_{max}] at each repetition.

Based on Shi and Eberhart (1998), we have defined the alteration of the *w* of the particle by a decreasing strategy linearly at each iteration in the following form:

$$w = \frac{1}{2}\left[w_{\max} - (w_{\max} - w_{\min}) \times \frac{t_{it}}{T_{\max}} \right] \quad (5)$$

where t_{it} is current iteration, and T_{max} is the maximum number of iterations.

Then, the fundamental procedure of PSO algorithm lies in quickening each individual towards its *Pbest* and the *Gbest* values with a random weighted acceleration at each iteration. It is worth noting that the maximum velocity (V_{max}) indicates the highest amount of location coordinates variation that can take place during each iteration. As a matter of fact, the concept of maximum velocity was introduced to avoid outflow and divergence (Das *et al.*, 2008).

When the differences between the observed gravity field data and the generated one from

the estimated model is minimised, the best exact values of the particles (model parameters) are obtained. For this purpose, we use the following simple objective function (Q):

$$Q = \frac{2\sum_{i}^{N}\left|g_i^o - g_i^c\right|}{\sum_{i}^{N}\left|g_i^o - g_i^c\right| + \sum_{i}^{N}\left|g_i^o + g_i^c\right|} \tag{6}$$

where N is the number of the gravity measurement point, g_i^o and g_i^c are the gravity anomaly observed and calculated at the point $P(x'_i)$, respectively.

The learning factors (c_1 and c_2) are traditionally both equal to 2 (Sweilam *et al.*, 2007). However, based on recent literature, electing c_1 more predominant than c_2 and $c_1 + c_2 \leq 4$ may present better conclusions (Parsopoulos and Vrahatis, 2002).

It can be observed that larger or smaller values of two factors c_1 and c_2 are not effective in the optimisation of parameters (Yi, 2016). For improving the proficiency of PSO, the values of two operators c_1 and c_2 are updated by two automatic linear expressions, respectively, at each iteration, as:

$$c_1 = 2.5 - \frac{0.5t_{it}}{T_{\max}} \tag{7}$$

$$c_2 = 1.5 + \frac{0.5t_{it}}{T_{\max}}. \tag{8}$$

With this strategy, learning factor c_1 can be decreased and learning factor c_2 can be increased with the addition of the number of iterations, as $c_1 + c_2 = 4$. The recovery of learning factors gradually reduces the trapping of the individual in local minima and improves the global search capability of particles in the whole search space and the ability to find the optimal solution when the number of iterations is increased. Fig. 2 shows the flowchart of MPSO.

4. Theoretical example

In this paper, the PSO and MPSO inversion process is repeated 50 and 10 times, respectively, by using a different initial population, and a model which having the least Q value (i.e. error) is selected as the best-fitting model. For all the synthetic models that will be investigated, according to the defined ranges for the parameters, one hundred primary models are randomly manufactured, as these ranges include the assumed values for the initial model. Moreover, the gravity sampling was performed with 5 m intervals along a 100 m profile. The number of iterations and allowable errors are assigned as 150 and 0.001 mGal, respectively. The variations of the search range for the q parameter is constant, i.e. $0.25 \leq q \leq 1.75$. The geometric shape of the anomaly causative body is determined considering the evaluated q using MPSO, as for $0.25 \leq q < 0.75$, $0.75 \leq q < 1.25$, and $1.25 \leq q \leq 1.75$ the buried mass shape is simulated as a vertical cylinder, horizontal cylinder, and sphere, respectively.

4.1. Sphere model

Fig. 3 (black circles) shows the computed theoretical gravity field variations due to a sphere model with the parameters h = 25 m and R = 10 m, where the maximum gravity is the centre of the profile. The density contrast is given as ρ = 2 g/cm^3. The search range for the parameters of the sphere model is indicated in Table 1. We have employed the MPSO algorithm to invert this theoretical gravity data. Figs. 4a to 4e demonstrate the variations of the z, R, q, ρ parameters and Q (error) values versus iteration number, respectively. The estimated final Q value is 0.013. The parameter values at the 126th iteration remain constant to the last iteration. The obtained values for the parameters are z = 25.19 m, R = 10.04 m, ρ = 2.03 g/cm^3, q = 1.52, and x_0 = 0 m (Table 1). The generated gravity from the resulted parameters by MPSO is shown in Fig. 3 (black curve).

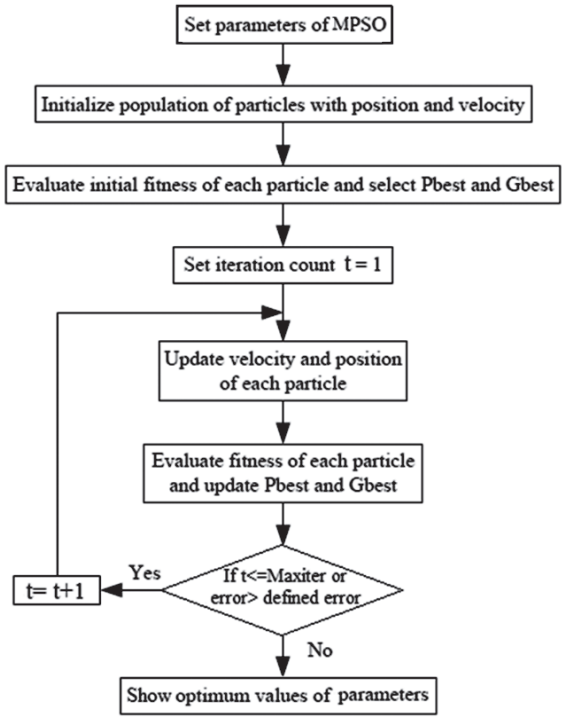

Fig. 2 - Flowchart of IPSO.

Table 1 - Initial assumptions and estimated numerical results for the noise-free and noise corrupted synthetic gravity anomaly of the sphere model.

Parameter		Q	z (m)	R (m)	ρ (g/cm^3)	q	x_0 (m)
Assumed		-	25	10	2.0	1.50	0
Ranges		-	10 to 40	1 to 20	0.5 to 3.5	0.25 to 1.75	-5 to 5
MPSO	Noise free	0.013	25.19	10.04	2.03	1.52	0
	10% noise	0.0275	26.13	11.18	2.10	1.58	0
PSO	Noise free	0.026	25.82	9.21	2.09	1.57	0
	10% noise	0.0782	22.40	12.33	2.47	1.65	-0.48

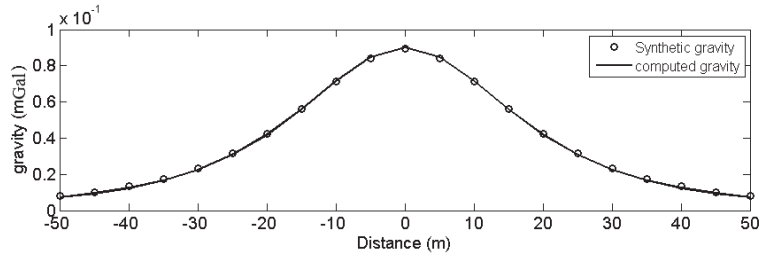

Fig. 3 - Synthetic gravity anomaly over the sphere model (circles) and generated gravity from the MPSO inversion (curve).

The ability of the MPSO algorithm is studied by adding 15% random noise to the gravity anomaly of the sphere model using the following equation:

$$g_{nois}(x_i) = g_{obs}(x_i)\{1 + [RAND(i) - 0.5]\times 0.15\} \quad (9)$$

where $g_{nois}(x_i)$ is the noise corrupted synthetic data at x_i, and *RAND(i)* is a pseudorandom number whose range is between 0 to 1.

Fig. 5 (black circles) shows the noise-corrupted theoretical gravity data of the sphere model. The variations of the *z*, *R*, ρ, *q* parameters and *Q* (error) values versus iteration number during inversion using MPSO are illustrated in Figs. 6a to 6e, respectively. The evaluated final *Q* value for the noisy gravity data related to the sphere model is 0.0275 as has been obtained at the 69th iteration. Thus, the values of the model parameter at the 69th iteration remain constant to the last iteration. Fig. 5 (curve) shows the generated gravity response by the inverted parameters from the contaminated synthetic gravity

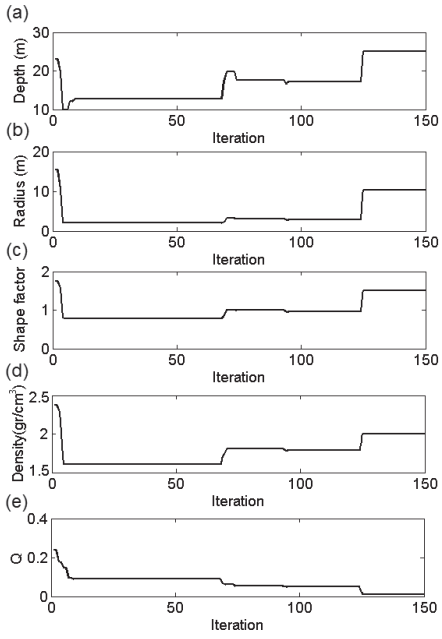

Fig. 4 - Variations of the *z*, *R*, *q*, ρ parameters and *Q* values versus iteration number for the synthetic gravity anomaly over the sphere model.

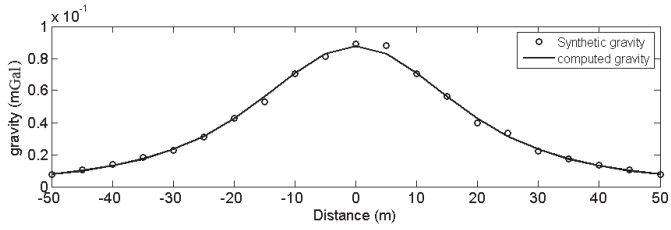

Fig. 5 - Synthetic gravity anomaly over the sphere model (circles) with 15% added noise and generated gravity from the MPSO inversion (curve).

data using MPSO whose values are *z* = 26.13 m, *R* = 11.80 m, ρ = 2.100 g/cm^3, *q* = 1.580, and x_0 = 0 m, as are indicated in Table 1. The PSO inversion of the gravity data due to this synthetic model estimated a *Q* error of 0.0260 and 0.0782 for noise-free and noisy gravity data, respectively, where these values were obtained at the last iteration (Table 1).

4.2. Horizontal cylinder model

The black circles in Fig. 7 demonstrate the theoretical gravity field variations over a horizontal cylinder model with the parameters *h* = 30 m and *R* = 15 m, where the maximum gravity is the centre of the profile. The density contrast is given as ρ = 1 g/cm^3. The search range for the parameters of the horizontal cylinder model is given in Table 2. We have employed the MPSO algorithm for inverting this theoretical gravity data. Figs. 8a to 8e show the variations of the *z*, *R*, *q*, ρ parameters and *Q* (error) values versus iteration number, respectively. The estimated final *Q* value is 0.018. The parameter values at the 29th iteration remain constant to the last iteration.

Table 2 - Initial assumptions and estimated numerical results for the noise-free and noise-corrupted synthetic gravity anomaly of the horizontal cylinder model.

Parameter		Q	z (m)	R (m)	ρ (g/cm^3)	q	x_0 (m)
Assumed		-	30	15	1	1	0
Ranges		-	10 to 50	5 to 30	0.5 to 3.0	0.25 to 1.75	-5 to 5
MPSO	Noise free	0.018	30.23	15.03	1.02	0.997	0
	10% noise	0.037	31.79	14.66	0.94	0.991	0
PSO	Noise free	0.031	30.84	15.63	1.08	1.062	0
	10% noise	0.0829	33.64	16.48	1.14	0.86	0.45

Thus, the best obtained values at the 29th iteration for the model parameters are z = 30.23 m, R = 15.03 m, ρ = 1.02 g/cm^3, q = 0.997, and x_0 = 0 m (Table 2). The generated gravity from the resulted parameters by MPSO is shown in Fig. 7 (black curve).

We have tested the efficiency of the MPSO algorithm in existence of noise. To this end**,** a set of 15% random noise based on Eq. 9, is distributed among the synthetic gravity data of the horizontal cylinder model.

Fig. 9 (black circles) shows the contaminated synthetic gravity data of the horizontal cylinder model. The variations of the z, R, ρ, q parameters and Q values versus iteration number during inversion using MPSO are displayed in Figs. 10a to 10e, respectively. The estimated final Q value for the noise-corrupted gravity data related to the horizontal cylinder model is 0.037 as has been obtained at the 145th iteration. Thus, the values of the model parameter at the 145th iteration remain unchanged to the last iteration. Fig. 9 (curve) shows the generated gravity response by the inverted parameters from the noisy theoretical gravity data using MPSO whose values are z = 31.79 m, R = 14.66 m, ρ = 0.94 g/cm^3, q = 0.991 and x_0 = 0 m, as are tabulated in Table 2. The Q errors estimated by PSO inversion of the gravity data due to horizontal cylinder model are 0.0310 and 0.0829 for noise-free and noisy gravity data, respectively, where these values were obtained at the last iteration (Table 2).

Table 3 - Initial assumptions and estimated numerical results for the noise-free and noise-corrupted synthetic gravity anomaly of the vertical cylinder model.

Parameter		Q	z (m)	R (m)	ρ (g/cm^3)	q	x_0 (m)
Assumed		-	40	12	1.5	0.5	0
Ranges		-	20 to 60	5 to 30	0.5 to 3.5	0.25 to 1.75	-5 to 5
MPSO	Noise free	0.0042	39.97	11.87	1.502	0.496	0
	10% noise	0.0170	40.45	12.74	1.57	0.511	0.27
PSO	Noise free	0.0740	40.82	12.69	1.54	0.508	0
	10% noise	0.2790	42.64	14.17	1.63	0.420	1.64

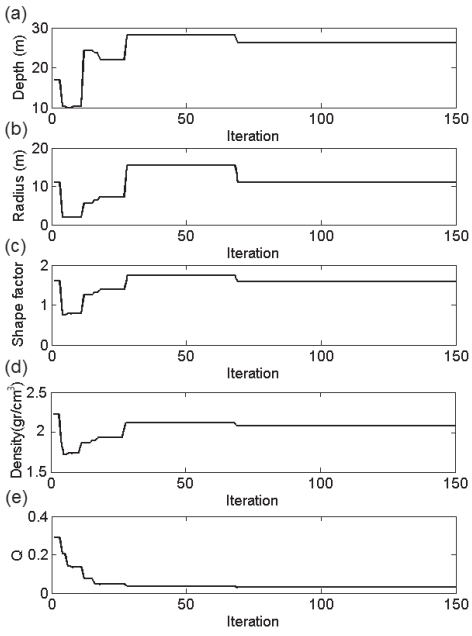

Fig. 6 - Variations of the z, R, q, ρ parameters and Q values versus iteration number for the noisy synthetic gravity anomaly over the sphere model.

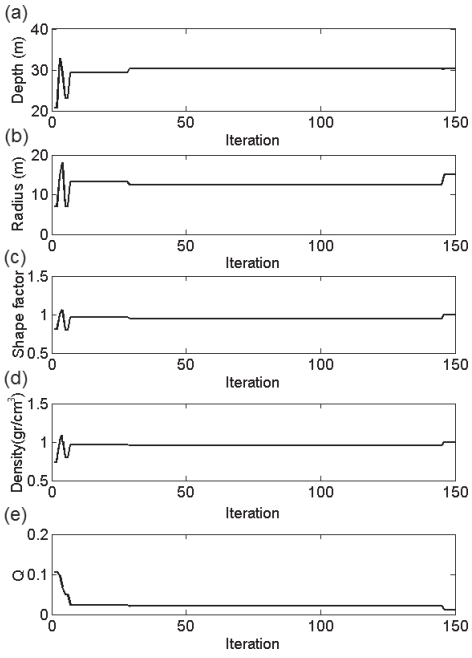

Fig. 8 - Variations of the z, R, q, ρ parameters and Q values versus iteration number for the synthetic gravity anomaly over the horizontal cylinder model.

4.3. Vertical cylinder model

The theoretical gravity field over a vertical cylinder model with the parameters h = 40 m and R = 12 m, where the maximum gravity is the centre of the profile, is demonstrated in Fig. 11 by the black circles. The density contrast is considered as ρ = 1.5 g/cm^3. The search range for the parameters of the vertical cylinder model is indicated in Table 3. We have also applied the MPSO algorithm for interpreting this theoretical gravity data. Figs. 12a to 12e present the variations of the z, R, q, ρ parameters and Q values versus iteration number,

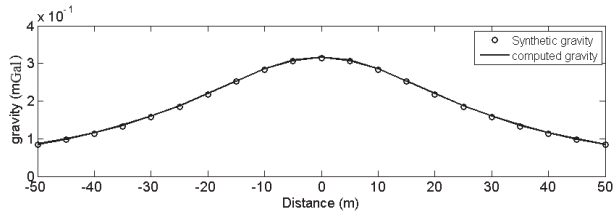

Fig. 7 - Synthetic gravity anomaly over the horizontal cylinder model (circles) and generated gravity from the MPSO inversion (curve).

respectively. The resulted final Q value is 0.0042. The parameter values at the 66th iteration remain constant to the last iteration. Thus, the best obtained solutions at the 66th iteration for the parameters of the vertical cylinder model are z = 39.97 m, R = 11.87 m, ρ = 1.502 g/cm^3, q = 0.496, and x_0 = 0 m (Table 3). The inverted gravity from the resulted parameters by MPSO is shown in Fig. 11 (black curve).

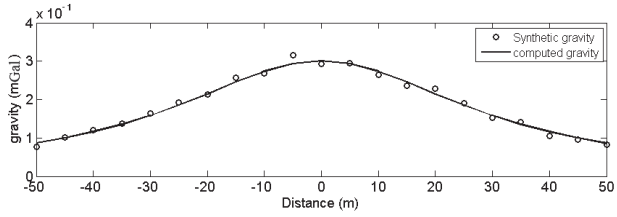

Fig. 9 - Synthetic gravity anomaly over the horizontal cylinder model (circles) with 15% added noise and generated gravity from the MPSO inversion (curve).

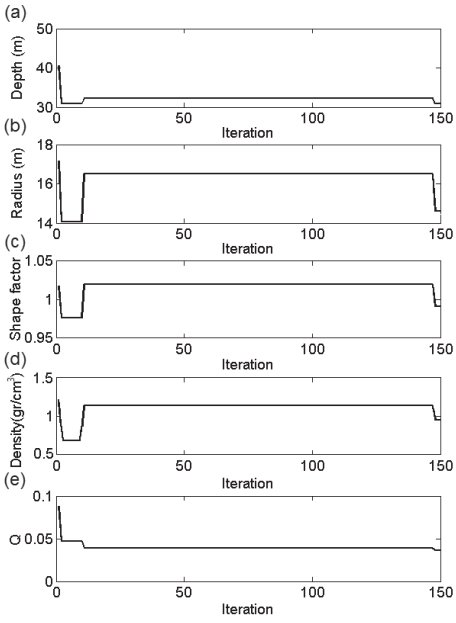

Fig. 10 - Variations of the z, R, q, ρ parameters and Q values versus iteration number for the noisy synthetic gravity anomaly over the horizontal cylinder model.

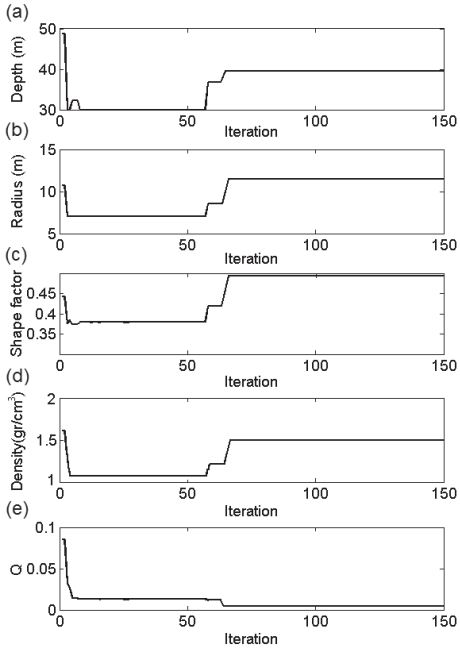

Fig. 12 - Variations of the z, R, q, ρ parameters and Q values versus iteration number for the synthetic gravity anomaly over the vertical cylinder model.

The effect of random noise on the MPSO algorithm efficiency has been investigated by adding 10% noise to the response of the vertical cylinder model (black circles in Fig. 11). For this purpose, in Eq. 9 we replaced 0.10 instead of 0.15.

Fig. 13 (black circles) shows the noise-corrupted synthetic gravity data of the vertical cylinder model. The variations of the z, R, ρ, q parameters and Q values versus iteration number during inversion using MPSO are indicated in Figs. 14a to 14e,

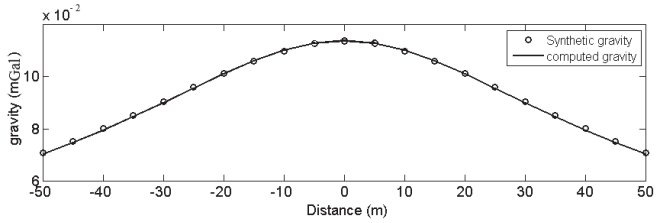

Fig. 11 - Synthetic gravity anomaly over the vertical cylinder model (circles) and generated gravity from the MPSO inversion (curve).

respectively. The inferred final Q value for the noise-corrupted gravity data related to the vertical cylinder model is 0.0137 as has been obtained at the 103th iteration. Therefore, the values of the model parameter at the 103th iteration remain unchanged to the last iteration. Fig. 13 (curve) shows the generated gravity response by the estimated parameters from the noisy theoretical gravity data using MPSO whose values are z = 40.45 m, R = 12.74 m, ρ = 1.57 g/cm^3, q = 0.511, and x_0 = 0.27 m, as are summarised in Table 3. The interpretation of the gravity data due to vertical cylinder model using PSO algorithm evaluated a Q error of 0.074 and 0.279 for noise-free and noisy gravity data, respectively,

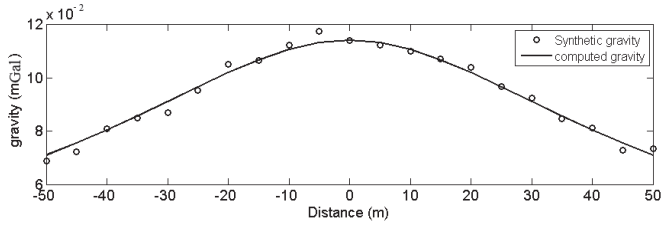

Fig. 13 - Synthetic gravity anomaly over the horizontal cylinder model (circles) with 15% added noise and generated gravity from the MPSO inversion (curve).

where these values were achieved at the last iteration (Table 3).

Table 4 - Parameters search range which are considered for the field examples.

Parameter Field example	z (m)	R (m)	ρ (g/m^3)	x_0 (m)
Humble Dome (USA)	2500 to 6500	1200 to 3200	-1.0 to -3.5	-1000 to 1000
Aqueduct (Tehran, Iran)	0.5 to 5.0	0.2 to 2.0	-1.0 to -3.5	-0.5 to 0.5
Bitumen (Dehloran, Iran)	5 to 50	5 to 25	-0.5 to -3.0	15 to 40
Chromite (Sabzevar, Iran)	2 to 15	2 to 25	0.5 to 3.5	-5 to 5
Leona (Saint-Louis, Senegal)	1500 to 6000	1000 to 3500	0.5 to 4.0	-1000 to 1000

5. Real gravity examples

In this paper, five real gravity data from various regions of the world are inverted using the MPSO algorithm and the estimated parameters are compared with results obtained from previous evaluations made by other inverse modelling methods.

Based on the assumed search ranges, 120 primary models are randomly considered for the causative mass of all the real gravity anomalies data. The number of iterations and permissible errors for the MPSO algorithm are determined as 150 and 0.005 mGal, respectively. The parameters search range for the regions under investigation are reported in Table 4. These defined boundaries have been chosen based on the geological information.

5.1. Humble Dome gravity anomaly, Texas, USA

The black circles in Fig. 15 show the residual gravity anomaly profile over the Humble Dome near Houston (Texas) that has been extracted from Nettleton (1976). The Humble Salt Dome is a significant geological structure for its oil and gas potential. The residual gravity anomaly over this salt dome was also interpreted by several authors and different methods, such as Shaw and Agarwal (1990), Abdelrahman *et al.* (2001), Tlas *et al.* (2005), Asfahani and Tlas (2012), Mehanee (2014), Biswas (2015), Singh and Biswas (2016), and Abdelrahman and Gobashy (2017). The results are summarised in Table 5.

Table 5 - Estimated parameters for the Humble Dome Anomaly, Texas, USA. Asterisks indicate the value of q that has been considered as a constant.

Parameter		z (m)	R (m)	ρ (g/m^3)	q	x_0 (m)
Researcher(s)	Method					
Tlas *et al.* (2005)	adaptive simulated annealing	4590	-	-	1.47	10
Asfahani and Tlas (2012)	fair function minimization	4580	-	-	1.48	-
Mehanee (2014)	simultaneous regularized inversion	4620	-	-	1.50*	-
Biswas (2015)	very fast simulated annealing	4400	-	-	1.50*	70
Singh and Biswas (2016)	global particle swarm optimization	4600±40	1937±573	2.050±1.260	1.50*	0.08±0.08
Abdelrahman and Gobashy (2017)	statistical approach	5050	-	-	1.40	-
Present method (MPSO)		4564	2100	-2.105	1.538	-18

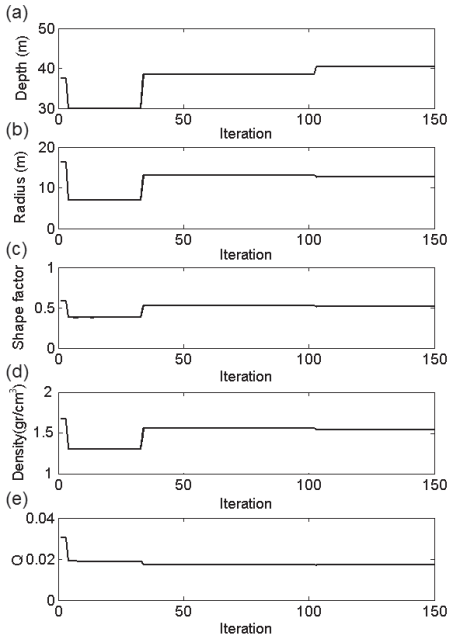

Fig. 14 - Variations of the *z*, *R*, *q*, *ρ* parameters and *Q* values versus iteration number for the noisy synthetic gravity anomaly over the vertical cylinder model.

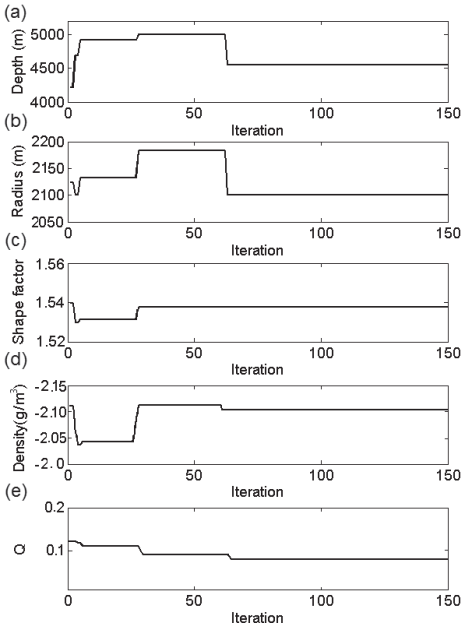

Fig. 16 - Variations of the *z*, *R*, *q*, *ρ* parameters and *Q* values versus iteration number for the gravity anomaly over the Humble Dome (USA).

We applied the MPSO for inverting the gravity anomaly profile over the Humble Dome where the residual gravity field has been digitised at 33 points with an interval of about 600 m along the profile. Figs. 16a to 16e show the variations of the *z*, *R*, *ρ*, *q* parameters and *Q* values versus iteration number during inversion, respectively. The least amount of the *Q* value is 0.076 mGal, which was acquired in the 67th iteration and this value remains invariable to the last iteration. The obtained values in the 67th iteration are Z = 4564 m, R = 2100 m, ρ = -2.105 g/m^3, q = 1.538, and x_0 = -18.00 m, as reported in Table 5. The produced gravity response by the estimated parameters using MPSO is shown in Fig. 15.

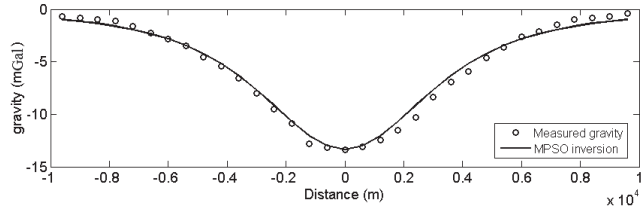

Fig. 15 - Observed gravity anomaly and MPSO inverted gravity anomaly due to the Humble Dome (USA).

5.2. Aqueduct gravity anomaly, Tehran, Iran

The black circles in Fig. 17 show a negative residual gravity anomaly measured over an aqueduct located in Tehran, Iran. The distance between the sampling stations is 0.2 m over a 2.2 m profile. The MPSO was used to find the optimal values of the parameters of the aqueduct structure. The variations of the model parameters and the error reduction versus the iteration number, which indicate the improvement of the structural parameter values, are shown in Figs. 18a to 18e. The minimum error with a value of 0.0067 mGal was estimated at the end of the 114th iteration and this value remained fixed to the last iteration. The estimated parameters at this iteration are z = 2.67 m, R = 0.84 m, ρ = -2.812 g/m^3, q = 1.07, and x_0 = -0.06 m, as these best solutions are reported in Table 6. The generated gravity from the computed parameters is shown in Fig. 17.

As expected, the estimated q = 1.07 illustrates the feature of the aqueduct is a horizontal cylinder and the evaluated density contrast shows

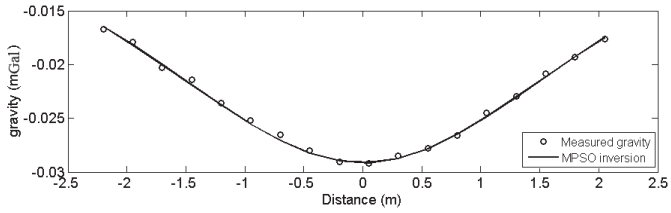

Fig. 17 - Observed gravity anomaly and MPSO inverted gravity anomaly due to the aqueduct (Tehran, Iran).

a good conformity with the mean density of the surrounding alluviums of the aqueduct. Moreover, the field investigations verify the accuracy of the calculated values for the parameters of the aqueduct structure.

Table 6 - Estimated parameters for the aqueduct gravity anomaly, Tehran, Iran.

Parameter	z (m)	R (m)	ρ (g/cm^3)	q	x_0 (m)
Present method (MPSO)	2.67	0.84	-2.812	1.07	-0.06

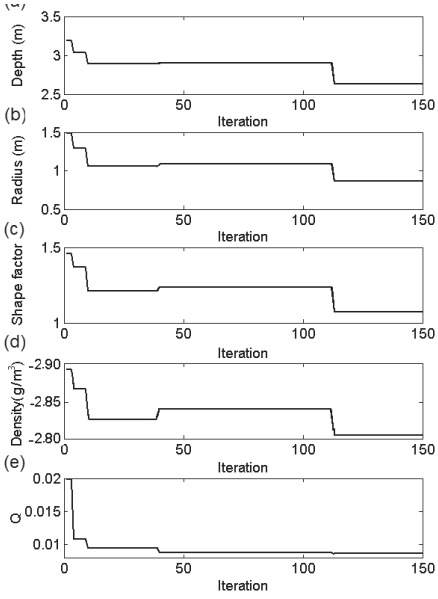

Fig. 18 - Variations of the z, R, q, ρ parameters and Q values versus iteration number for the gravity anomaly over the aqueduct (Tehran, Iran).

5.3. Bitumen deposit gravity anomaly, Dehloran, Iran

The black circles in Fig. 19 show the residual gravity anomaly profile due to a bitumen deposit, which is located in west of Iran in the Zagros tectonic zone. One of the most considerable specificities of this region is its hydrocarbon potential. The gravity data are sampled at 25 points, over 60 m profile with a 2.5 m interval. This field anomaly has previously been analysed by Abedi *et al.* (2010) and Tlas and Asfahani (2018). We have inverted this residual gravity anomaly using proposed method. Figs. 20a to 20e show the variations of the z, R, ρ, q parameters and Q values versus iteration number during inversion, respectively. The values of the inferred parameters for the buried bitumen deposit are z = 25.21 m, R = 13.20 m, ρ = -1.340 g/m^3, q = 0.96, and x_0 = 27.85 m, which are tabulated in Table 7. The generated gravity of the MPSO inversion response is also shown in Fig. 19 with a black curve.

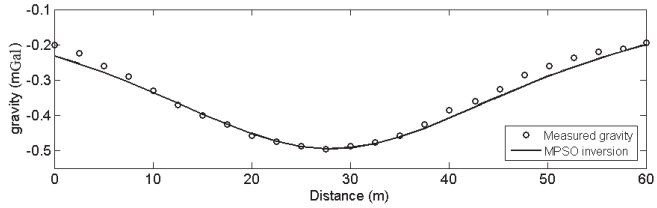

Fig. 19 - Observed gravity anomaly and MPSO inverted gravity anomaly due to the bitumen deposit (Dehloran, Iran).

Table 7 - Estimated parameters for the bitumen deposit gravity anomaly, Dehloran, Iran. Asterisks indicate the value of *q* that has been considered as a constant.

Parameter		*z* (m)	*R* (m)	*ρ* (g/m³)	*q*	x_0 (m)
Researchers	Method					
Abedi *et al.* (2010)	Normalized method	23.73	-	-	1*	-
	Least-squares minimisation	23.31	14.1	-	1*	-
	Neural network modelling	22.80	13.8	-	1*	-
Tlas and Asfahani (2018)	quadratic curve regression	24.59	-	-	1*	27.62
Present method (MPSO)		25.21	13.2	-1.340	0.96	27.85

The least amount of the *Q* whose value is 0.051 mGal (minimum error) was obtained at the end of the 68th iteration and this value remains unchanged to the last iteration (Fig. 20e).

Considering the density contrast between bitumen and the dominant surrounding formations (layers of limestone with intermediate marl-limestone) in this region, which is about -1.40 g/cm³, the density contrast -1.34 g/cm³ estimated by MPSO is wholly acceptable.

5.4. Chromite deposit gravity anomaly, Sabzevar, Iran

Fig. 21 represents the residual gravity anomaly map of an area under investigation in Sabzevar, Iran. The 22 black circles in Fig. 22 show the residual gravity field variations related to a subsurface chromite mass measured along profile AB, as shown in Fig. 21. The length of the profile AB is 42 m and gravity data sampling interval is 2 m. The average density of the chromite mass is about 4.6 g/cm³, whereas the density of the surrounding formation is about 3 g/cm³. Consequently, the density contrast between the chromite ore body and surrounding formation is about 1.6 g/cm³.

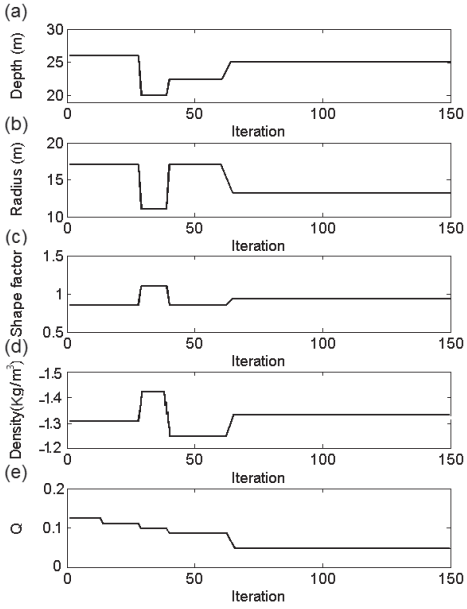

Fig. 20 - Variations of the *z*, *R*, *q*, *ρ* parameters and *Q* values versus iteration number for the gravity anomaly over the bitumen deposit (Dehloran, Iran).

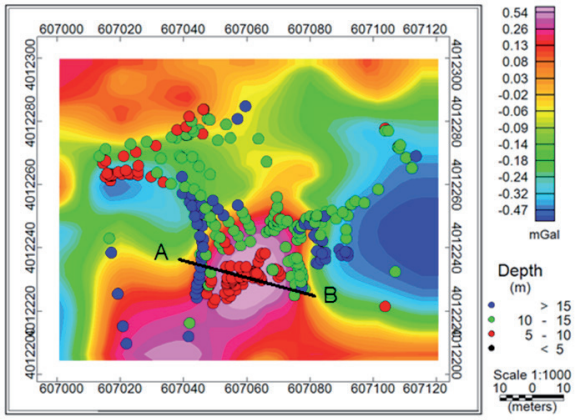

Fig. 21 - The residual gravity anomalies overlaid by depth solutions of the 3D Euler method.

Table 8 - Estimated parameters for the chromite deposit gravity anomaly, Sabzevar, Iran. Asterisks indicate the value of *q* that has been considered as a constant.

Parameter		*z* (m)	*R* (m)	ρ (g/m^3)	*q*	x_0 (m)
Researchers	Method					
Eshaghzadeh *et al.* (2019)	Forced Neural Network	8.00	9.00	-	0.5*	-
Eshaghzadeh *et al.* (2019)	Marquardt's algorithm	7.50	11.70	-	0.5*	-
Present method (MPSO)		5.98	14.62	1.786	0.598	0.12

Eshaghzadeh *et al.* (2019) interpreted this anomaly in two separate papers using the forced neural network and Marquardt's algorithm (Marquardt, 1963) methods (see Table 8). Here, we have employed the MPSO algorithm to invert the chromite deposit gravity anomaly. Figs. 23a to 23e display the variations of the *z*, *R*, ρ, *q* parameters and *Q* values versus iteration number during MPSO inversion. The best values of the inferred parameters for the ore body structure, which was acquired at the end of the 62th iteration with an error value of 0.082 mGal, are *z* = 5.98 m, *R* = 14.62 m, ρ = 1.786 g/m^3, *q* = 0.598, and x_0 = 0.12 m, as reported in Table 8. The black curve in Fig. 22 shows the gravity response according to these estimated parameters. As seen, the resulted density contrast has an acceptable accordance with the density contrast of the region under investigation.

The Euler deconvolution method is a common technique in potential fields study, and is widely used for estimating the depth of the anomaly source (Reid *et al.*, 1990; Silva and Barbosa, 2003). For comparison, we have employed the Euler method to calculate the depth of the chromite mineral mass by choosing a structure index of 1 and a window size of 5×5 points. Fig. 21 shows the solutions obtained from the Euler deconvolution as plotted on the residual gravity anomaly

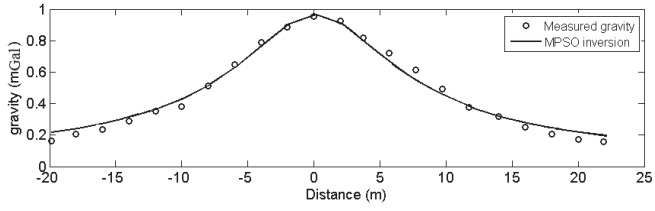

Fig. 22 - Observed gravity anomaly and MPSO inverted gravity anomaly due to the chromite deposit (Sabzevar, Iran).

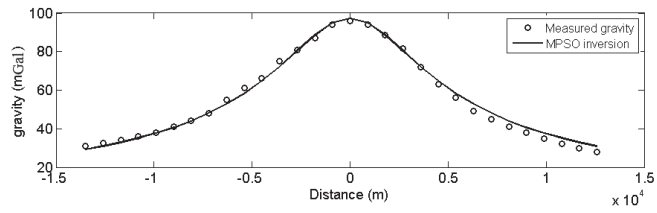

Fig. 24 - Observed gravity anomaly and MPSO inverted gravity anomaly due to the Leona deposit (south of Saint-Louis, Senegal).

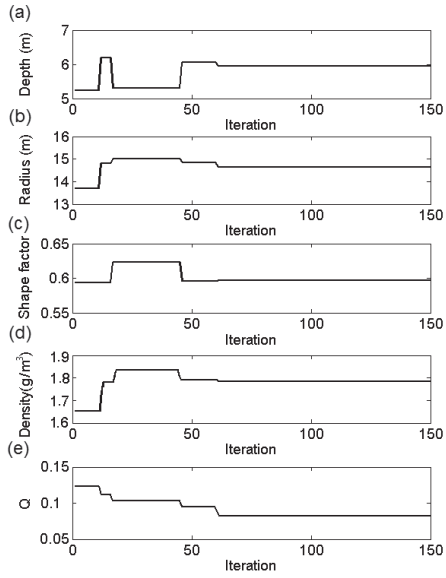

Fig. 23 - Variations of the *z*, *R*, *q*, ρ parameters and *Q* values versus iteration number for the gravity anomaly over the chromite deposit (Sabzevar, Iran).

map. The Euler solutions located on the gravity anomaly present a depth between 5 to 10 m for the buried deposit. There is a satisfactory agreement between the computed depths by the MPSO algorithm and Euler deconvolution method.

5.5. Leona gravity anomaly, south of Saint-Louis, Senegal

We have digitalised the residual gravity data at 30 points with an equal interval of 900 m, from over a measured gravity profile of 30 km in the west coast of Senegal, taken from Nettleton (1976). This field anomaly has previously been evaluated by Tlas *et al.* (2005), Asfahani and Tlas (2012), Mehanee (2014), Biswas (2015), and Singh and Biswas (2016). This extracted anomaly is illustrated in Fig. 24 with the black circles. This region has been surveyed for its oil and gas potential. The MPSO was also utilised to analyse this anomaly. The optimal solutions for the parameters have been gained at the end of the 141th iteration, as the Q reaches its minimum value, that is 0.036 mGal, and this value remains unchanged to the last iteration. The variations of the z, R, ρ, q parameters and Q values versus iteration number during inversion using MPSO are shown in Figs. 25a to 25e, respectively. The estimated values for the buried structure parameters are z = 3821 m, R = 1935 m, ρ = 2.343 g/m^3, q = 0.464, and x_0 = -114 m, as reported in Table 9, which can compare with other method's outputs. The gravity response due to evaluated parameters is shown in Fig. 24.

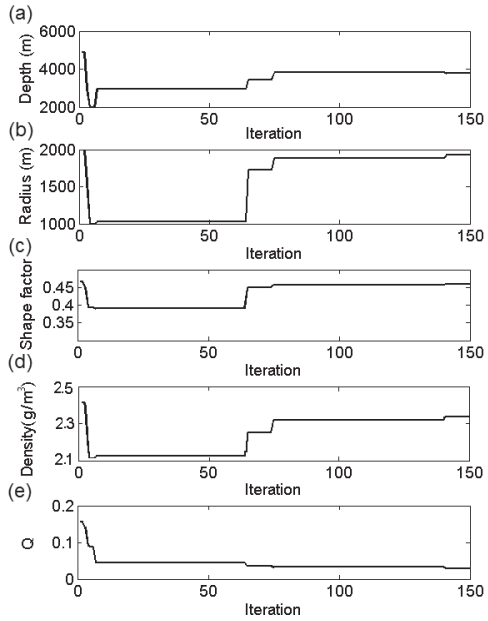

Fig. 25 - Variations of the z, R, q, ρ parameters and Q values versus iteration number for the gravity anomaly over the Leona deposit (south of Saint-Louis, Senegal).

Table 9 - Estimated parameters for the Leona deposit gravity Anomaly, south of Saint-Louis, Senegal. Asterisks indicate the value of q has been considered as a constant.

Parameter		***z* (m)**	***R* (m)**	***ρ* (g/m^3)**	***q***	***x*$_0$ (m)**
Researchers	Method					
Tlas *et al.* (2005)	adaptive simulated annealing	9170	-	-	1.499	220
Asfahani and Tlas (2012)	fair function minimization	9130	-	-	1.499	-
Mehanee (2014)	simultaneous regularized inversion	12200	-	-	1.5*	-
	simultaneous regularized inversion	4590	-	-	0.5*	-
Biswas (2015)	very fast simulated annealing	4600	-	-	0.5*	-400
Singh and Biswas (2016)	global particle swarm optimization	4500±1780	33050±799	2.370±0.980	0.5*	-240±50
Present method (MPSO)		3821	1935	2.343	0.464	-114

6. Conclusions

Presence of errors in geophysical inverse modelling and numerical computation is unavoidable, due to some factors such as the heterogeneity and discontinuity of the interior geological structures, the incoherence and incompatibility of the undersurface structures, and masses configuration with various geometric shapes. Therefore, the proposed method is no exception as well. However, determining the minimum and maximum values for the variables based on the geological and geophysical information, which is an important advantage in the MPSO approach over many of the nonlinear inversion methods, can notably decrease the computational error. However, many of the assumed initial values for the idealised source parameters are more accurate, the convergence rate of the MPSO is faster.

In this paper, we have introduced the MPSO algorithm as an automatic powerful tool for solving the multivariable problem. MPSO is a mathematical process that tries to fit theoretical gravity anomalies with observed ones by improving the buried structure parameters. For this method, a flexible code has been written to consider the estimated shape factor at each iteration as the forward modelling is performed.

The method was examined on synthetic gravity data with and without random noise for three synthetic idealised models. The obtained admissible results from the inversion verify the MPSO is an intelligent technique for the inverse modelling of the gravity field.

For comparison, we also applied the PSO algorithm to interpret the synthetic models. The results show that the MPSO algorithm is faster than the PSO algorithm and the iteration number for convergence of responses in MPSO is less than PSO. Moreover, the accuracy of obtained results from the MPSO is better than PSO. Because PSO sticks to the local minimum during inversion, the number of the repetition times of the PSO algorithm is more than the MPSO method.

MPSO was applied to analyse the five real residual gravity data profiles from Iran, USA, and Senegal. The estimated parameters for the subsurface causative mass using MPSO inversion was also compared with ones obtained from other methods proposed by several researchers. Based on the fact that the resulting shape factors can simulate the geometrical shape of the gravity anomaly sources of the case studies, i.e. the Humble Dome (q = 1.538), aqueduct (q = 1.070), bitumen (q = 0.960), chromite (q = 0.598), Leona (q = 0.464), the shape of the Humble Dome is, therefore, a sphere, the aqueduct structure and bitumen are horizontal cylinder forms, and the chromite deposit and Leona structure are vertical cylinder forms.

REFERENCES

Abdelrahman E.M.; 1990: *Discussion on "A least-squares approach to depth determination from gravity data" by O.P. Gupta*. Geophys., 55, 376-378.

Abdelrahman E.M. and El-Araby H.M.; 1993a: *A least-squares minimization approach to depth determination from moving average residual gravity anomalies*. Geophys., 59, 1779-1784.

Abdelrahman E.M. and El-Araby H.M.; 1993b: *Shape and depth solutions from gravity using correlation factors between successive least-squares residuals*. Geophys., 59, 1785-1791.

Abdelrahman E.M. and Gobashy M.; 2017: *Depth and shape solutions from residual gravity anomalies due to simple geometric structures using a statistical approach*. Contrib. Geophys. Geod., 47, 113-132, doi: 10.1515/congeo-2017-0008.

Abdelrahman E.M., Bayoumi A.L., Abdelhady Y.E., Gobashy M.M. and El-Araby H.M.; 1989: *Gravity interpretation using correlation factors between successive least-squares residual anomalies*. Geophys., 54, 1614-1621.

Abdelrahman E.M., Bayoumi A.L. and El-Araby H.M.; 1991: *A least-squares minimization approach to invert gravity data*. Geophys., 56, 115-l18, doi: 10.1190/1.1442946.

Abdelrahman E.M., El-Araby T.M., El-Araby H.M. and Abo-Ezz E.R.; 2001: *Three least squares minimization approaches to depth, shape, and amplitude coefficient determination from gravity data*. Geophys., 66, 1105-1109.

Abedi M., Afshar A., Ardestani V.E., Norouzi G.H. and Lucas C.; 2010: *Application of various methods for 2D inverse modelling of residual gravity anomalies*. Acta Geophys., 58, 317-336.

Al-Garni M.A.; 2013: *Inversion of residual gravity anomalies using Neural Network*. Arabian. J. Geosci., 6, 1509-1516.

Asfahani J. and Tlas M.; 2008: *An automatic method of direct interpretation of residual gravity anomaly profiles due to spheres and cylinders*. Pure Appl. Geophys., 165, 981-994.

Asfahani J. and Tlas M.; 2012: *Fair function minimization for direct interpretation of residual gravity anomaly profiles due to spheres and cylinders*. Pure Appl. Geophys., 169, 157-165.

Biswas A.; 2015: *Interpretation of residual gravity anomaly caused by a simple shaped body using very fast simulated annealing global optimization*. Geosci. Front., 6, 875-893, doi: 10.1016/j.gsf.2015.03.001.

Bowin C., Scheer E. and Smith W.; 1986: *Depth estimates from ratios of gravity, geoid, and gravity gradient anomalies*. Geophys., 51, 123-136.

Chakravarthi V. and Sundararajan N.; 2004: *Ridge regression algorithm for gravity inversion of fault structures with variable density*. Geophys., 69, 1394-1404.

Das S., Abraham A. and Konar A.; 2008: *Particle swam optimization and differential evolution algorithms: technical analysis, applications and hybridization perspectives*. Stud. Comput. Intell., 116, 1-38.

Eshaghzadeh A. and Kalantary R.A.; 2015: *Anticlinal structure modelling with Feed forward Neural Networks for residual gravity anomaly profile*. In: Proc., 8th Congress of the Balkan Geophysical Society, Chania, Greece, Vol. 2015, pp. 1-5, doi: 10.3997/2214-4609.201414210.

Eshaghzadeh A. and Hajian A.; 2018: *2D inverse modelling of residual gravity anomalies from simple geometric shapes using Modular Feed-forward Neural Network*. Ann. Geophys., 61, SE115, 9 pp., doi: 10.4401/ag-7540.

Eshaghzadeh A., Dehghanpour A. and Sahebari S.S.; 2019: *Marquardt inverse modelling of the residual gravity anomalies due to simple geometric structures: a case study of chromite deposit*. Contrib. Geophys. Geod., 49, 153-180.

Eshaghzadeh A., Sahebari S.S. and Dehghanpour A.; 2020: *2D inverse modelling of the gravity field due to a chromite deposit using the Marquardt's algorithm and Forced Neural Network*. Bull. Miner. Res. Explor., 161, 33-47.

Eslam E., Salem A. and Ushijima K.; 2001: *Detection of cavities and tunnels from gravity data using a Neural Network*. Explor. Geophys., 32, 204-208.

Essa K.S.; 2007: *A simple formula for shape and depth determination from residual gravity anomalies*. Acta Geophys., 55, 182-190.

Essa K.S. and El-Hussein M.; 2017: *2D dipping dike magnetic data interpretation using a robust particle swarm optimization*. Geosci. Instrum. Method Data Syst., 39**,** 10 pp. doi: 10.5194/gi-2017-39.

Essa K.S. and El-Hussein M.; 2018a: *Gravity data interpretation using different new algorithms: a comparative study*. In: Zouaghi T. (ed), Gravity - Geoscience Applications, Industrial Technology and Quantum Aspect, Chapter 1, pp. 1-17, Books on Demand, Nordersteat, Germany, doi: 10.5772/intechopen.71086.

Essa K.S. and El-Hussein M.; 2018b: *PSO (Particle Swarm Optimization) for interpretation of magnetic anomalies caused by simple geometrical structures*. Pure Appl. Geophys., 175, 3539-3553.

Fernandez Alvarez J.P., Fernandez Martinez J.L., Garcia Gonzalo E. and Menendez Perez C.O.; 2006: *Application of the Particle Swarm Optimization (PSO) algorithm to the solution and appraisal of the VES inverse problem*. In: Proc., 11th Annual Conference of the International Association of Mathematical Geology (IAMG06), Liege, Belgium, pp. S12-S17.

Gupta O.P.; 1983: *A least-squares approach to depth determination from gravity data*. Geophys., 48, 357-360.

Hammer S.; 1977: *Graticule spacing versus depth discrimination in gravity interpretation*. Geophys., 42, 60-65.

Kennedy J. and Eberhart R.; 1995: *Particle swarm optimization*. In: Proc., International Conference on Neural Networks, Perth, WA, Australia, Vol. 4, pp. 1942-1948, doi: 10.1109/ICNN.1995.488968.

Lines L.R. and Treitel S.; 1984: *A review of least-squares inversion and its application to geophysical problems*. Geophys. Prospect., 32, 159-186.

Marquardt D.W.; 1963: *An algorithm for least-squares estimation of nonlinear parameters*. J. Soc. Indian Appl. Math., 11, 431-441.

Mehanee S.A.; 2014: *Accurate and efficient regularized inversion approach for the interpretation of isolated gravity anomalies*. Pure Appl. Geophys., 171, 1897-1937.

Mohan N.L., Anandababu L. and Rao S.; 1986: *Gravity interpretation using the Melin transform*. Geophys., 51, 114-122.

Monteiro Santos F.A.; 2010: *Inversion of self-potential of idealized bodies' anomalies using particle swarm optimization*. Comput. Geosci., 36, 1185-1190.

Nettleton L.L.; 1976: *Gravity and magnetics in oil prospecting*. McGraw-Hill Book Inc., New York, NY, USA, 480 pp.

Odegard M.E. and Berg J.W.; 1965: *Gravity interpretation using the Fourier integral*. Geophys., 30, 424-438.

Osman O., Muhittin A.A. and Ucan O.N.; 2006: *A new approach for residual gravity anomaly profile interpretations: Forced Neural Network (FNN)*. Ann. Geophys., 49, 1201-1208.

Osman O., Muhittin A.A. and Ucan O.N.; 2007: *Forward modelling with Forced Neural Networks for gravity anomaly profile*. Math. Geol., 39, 593-605.

Pallero J.L.G., Fernández-Martínez J.L., Bonvalot S. and Fudym O.; 2015: *Gravity inversion and uncertainty assessment of basement relief via Particle Swarm Optimization*. J. Appl. Geophys., 116, 180-191.

Parsopoulos K.E. and Vrahatis M.N.; 2002: *Recent approaches to global optimization problems through particle swarm optimization*. Nat. Comput., 1, 235-306.

Reid A.B., Allsop J.M., Granser H., Millet A.J. and Somerton I.W.; 1990: *Magnetic interpretation in three dimensions using Euler deconvolution*. Geophys., 55, 80-91.

Roshan R. and Singh U.K.; 2017: *Inversion of residual gravity anomalies using tuned PSO*. Geosci. Instrum. Method Data Syst., 6, 71-79.

Saxov S. and Nygaard K.; 1953: *Residual anomalies and depth estimation*. Geophys., 18, 913-928.

Sharma B. and Geldart L.P.; 1968: *Analysis of gravity anomalies of two-dimensional faults using Fourier transforms*. Geophys. Prosp., 16, 77-93, doi: 10.1111/j.1365-2478.1968.tb01961.x.

Shaw R.K. and Agarwal N.P.; 1990: *The application of Walsh transforms to interpret gravity anomalies due to some simple geometrically shaped causative sources: a feasibility study*. Geophys., 55, 843-850.

Shaw R. and Srivastava S.; 2007: *Particle Swarm Optimization: a new tool to invert geophysical data*. Geophys., 72, F75-F83.

Shi Y. and Eberhart R.; 1998: *Parameter selection in Particle Swarm Optimization*. In: Proc., 7th Annual Conference on Evolutionary Programming, San Diego, CA, USA, pp. 591-601.

Silva J.B.C. and Barbosa V.C.F.; 2003: *3D Euler deconvolution: theoretical basis for automatically selecting good solutions*. Geophys., 68, 1962-1968.

Singh A. and Biswas A.; 2016: *Application of global particle swarm optimization for inversion of residual gravity anomalies over geological bodies with idealized geometries*. Nat. Resour. Res., 25, 297-314.

Singh K.K. and Singh U.K.; 2017: *Application of particle swarm optimization for gravity inversion of 2.5-D sedimentary basins using variable density contrast*. Geosci. Instrum. Method Data Syst., 6, 193-198.

Sweilam N.H., El-Metwally K. and Abdelazeem M.; 2007: *Self potential signal inversion to simple polarized bodies using the particle swarm optimization method: a visibility study*. J. Appl. Geophys., 6, 195-208.

Tlas M. and Asfahani J.; 2018: *Interpretation of gravity anomalies due to simple geometric-shaped structures based on quadratic curve regression*. Contrib. Geophys. Geod., 48, 161-178.

Tlas M., Asfahani J. and Karmeh H.; 2005: *A versatile nonlinear inversion to interpret gravity anomaly caused by a simple geometrical structure*. Pure Appl. Geophys., 162, 2557-2571.

Toushmalani R.; 2013a: *Comparison result of inversion of gravity data of a fault by particle swarm optimization and Levenberg-Marquardt methods*. SpringerPlus, 2, 462, doi: 10.1186/2193-1801-2-462.

Toushmalani R.; 2013b: *Gravity inversion of a fault by Particle Swarm Optimization (PSO)*. SpringerPlus, 2, 315, doi: 10.1186/2193-1801-2-315.

Yi L.; 2016: *Study on an improved PSO algorithm and its application for Solving Function Problem*. Int. J. Smart Home, 3, 51-62.

Corresponding author: Ata Eshaghzadeh (ORCID: 0000-0003-0665-0517)
Department of Geology, Faculty of Sciences, University of Isfahan
Azadi square, Isfahan, Iran
Phone: +98 11 5228 6946; e-mail: eshagh@alumni.ut.ac.ir